Supplementary information

A Heterostructure Topology of Hexagonal $BaTiO_3$ for Toluene Detection Using a 2D SnO based Chemiresistive Sensor

Anshika Singh[1*], Ravindra Kumar Rawat[*], Atul Kumar, Pratima Chauhan[*]

Advanced Nanomaterials Research Laboratory, U.G.C. Centre of Advanced Studies, Department of Physics, University of Allahabad, Prayagraj, Uttar Pradesh, 211002, India

[1]Present Address: SAMTEL Centre for Display Technologies, Indian Institute of Technology Kanpur, Uttar Pradesh, 208016, India

Corresponding Author E-mail id: anshikasingh@allduniv.ac.in; ravindrarawat@allduniv.ac.in; mangu167@yahoo.co.in

Characterization Tools

Rigaku Smart Lab X-ray Diffractometer used for the structural analysis of the $BaTiO_3$ and SnO samples. The TECNAI G20 High-Resolution Transmission Electron Microscope (HRTEM) and JEOL JSM-7610F Field Emission Scanning Electron Microscope (FESEM) was used to carried out surface morphological analysis. The sensing measurements were carried out through the Keithley 2182A nanovoltmeter and Keithley 6221 current source. During the observations, the applied voltage difference and current were 10 V and 20 μA, respectively. The reducing volatile organic compound gases were created by evaporating their liquid forms in a hot testing chamber. With the help of static liquid gas diffusion method, the concentration (C) of the test gases were calculated by the following formula:

$$\textbf{C (ppm)} = \frac{22.4 \times V_1 \times \emptyset \times \rho}{V_2 \times M} \times 1000$$

where C, V_1, $\emptyset$, ρ, M and V_2 denote the concentration of the target gas, volume of the liquid, target gas volume fraction, density of the liquid, molecular weight of liquid and volume of the testing chamber, respectively.[45] For reductive analyte, sensor response was calculated by the formula mentioned:

$$S = \frac{(R_{air} - R_{gas})}{R_{gas}} \times 100$$

where R_{air} and R_{gas} represent the resistances of the sensor in the presence of air and reducing gas, respectively.[19] Moreover, the response and recovery time of the sensor are defined as the temporal length of the event taken by the sensor to achieve 10 % to 90 % of the maximum resistance change in the case of adsorption and desorption, respectively. The temperature and relative humidity (RH) at ambient condition was 25 ℃ and 65 %, respectively.

XRD Analysis

The crystallite size of the $BaTiO_3$ and SnO are determined by the Scherrer formula:

$$D = \frac{0.98\,\lambda}{\beta cos\theta}$$

where D is the crystallite size in nanometre, λ is the wavelength of the incident radiation of Cu K_α (0.15406 nm), β is the FWHM and θ is Bragg's angle. The crystallite size of the $BaTiO_3$ and SnO found to be 29.48 and 26.42 nm.

BET analysis

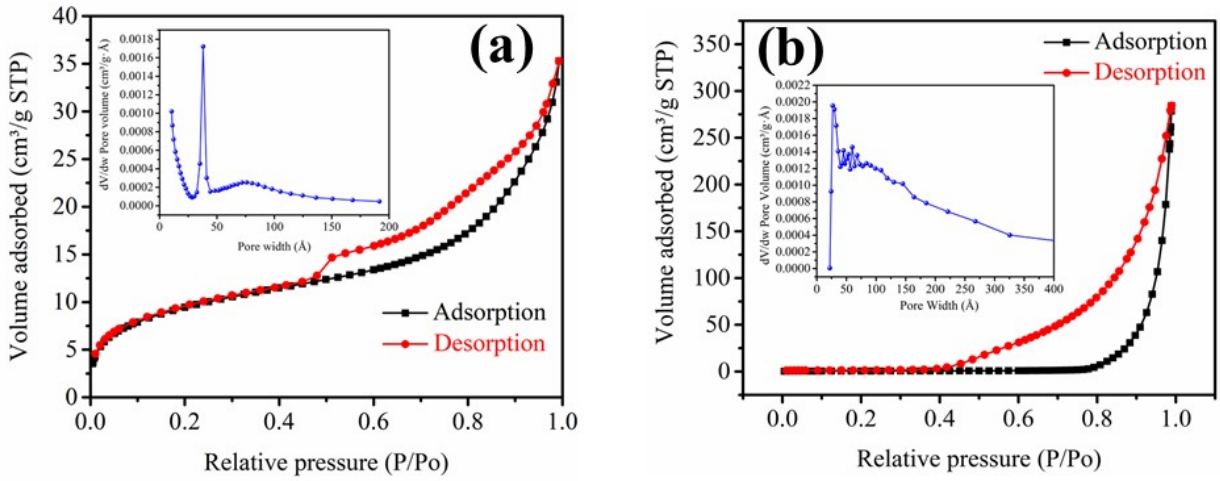

Fig. S1 ((a) and (b)) represent the N_2 adsorption-desorption isotherm and BJH-derived pore size distribution (inset) of the SnO and $BaTiO_3$, respectively.

Sensing Measurements

Thus, the investigation of single layered $BaTiO_3$ based device for VOCs at room temperature has its own importance. The gas molecules interaction path of the device protocol#1 and selectivity of the single layer $BaTiO_3$ device as given in Fig. S2. From the bar diagram, it is clear that the device doesn't respond to VOCs, but it can be useful as a humidity-sensing device. The response of the single-layered $BaTiO_3$ device towards the 95 % RH was ~76 %, which is

caused by the chemisorption and physisorption of water molecules over the surface of $BaTiO_3$. In the bilayered device protocol, the SnO and $BaTiO_3$ are spin-coated layer-by-layer over IDEs (Protocol#2 and Protocol#3).

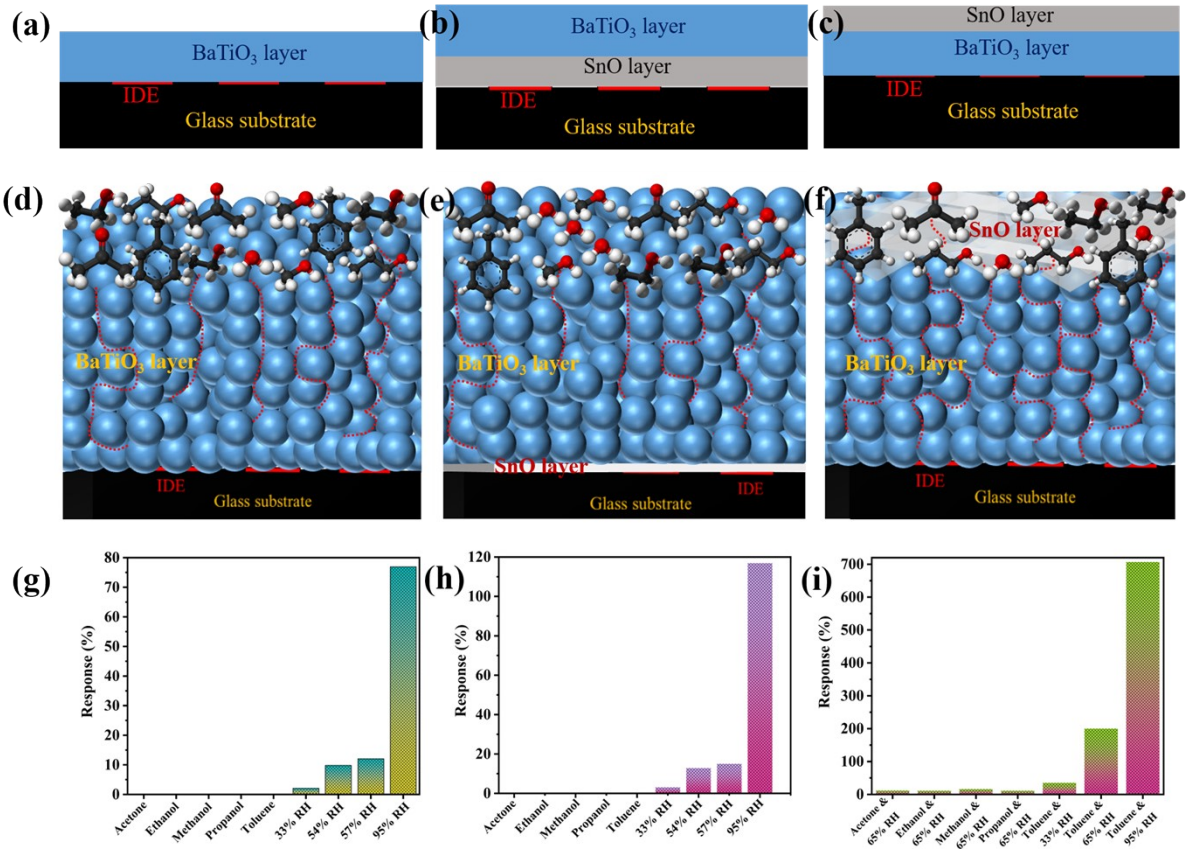

Fig. S2 (a), (b) and (c) represent the device structure, VOCs and water interaction schematics and selectivity of the device for protocol#1 ($BaTiO_3$ only), respectively; (d), (e) and (f) show the device structure, VOCs and water interaction schematics and selectivity of the device for protocol#3 ($BaTiO_3$-SnO), respectively; similarly (g), (h) and (i) show the device structure, VOCs and water interaction schematics and selectivity of the device for protocol#2 (SnO-$BaTiO_3$), respectively.

For the gas sensing purpose, both devices were investigated under VOCs atmospheres and different RH levels. The device protocol#2, targeted molecules interaction paths and selectivity of the device as presented in Fig. S2. This device (protocol#2) possessed the response towards the VOCs as well as water. The response of the device towards the various VOCs was observed at ambient conditions. The responses of the device towards the ethanol, methanol, propanol, acetone and toluene at 500 ppm and 65 % RH were ~11 %, ~16 %, ~11 %, ~12 % and ~200 %, respectively. Moreover, the response of the device under 33% RH and 95% RH with 500

ppm toluene concentration were ~35 % and ~562 %, respectively. For device protocol#2, toluene gas was selected for further investigation. The device protocol#3, targeted molecules interaction paths and selectivity of the device as shown in Fig. S2. The response bar diagram of device protocol#3 reveals that the device possessed excellent performance towards the various humidity levels. The response of the device towards the 33 % RH, 54 % RH, 57 % RH and 95 % RH were ~3 %, ~12 %, ~15 %, and ~116 %, respectively. From Fig. S2 it is pointed out that device protocol#2 is more significant in the case of VOCs as well as humidity sensing. In a comparative study with acetone, ethanol, methanol, propanol and toluene, device protocol#2 shows the highest response towards toluene, as shown in Fig. S2.

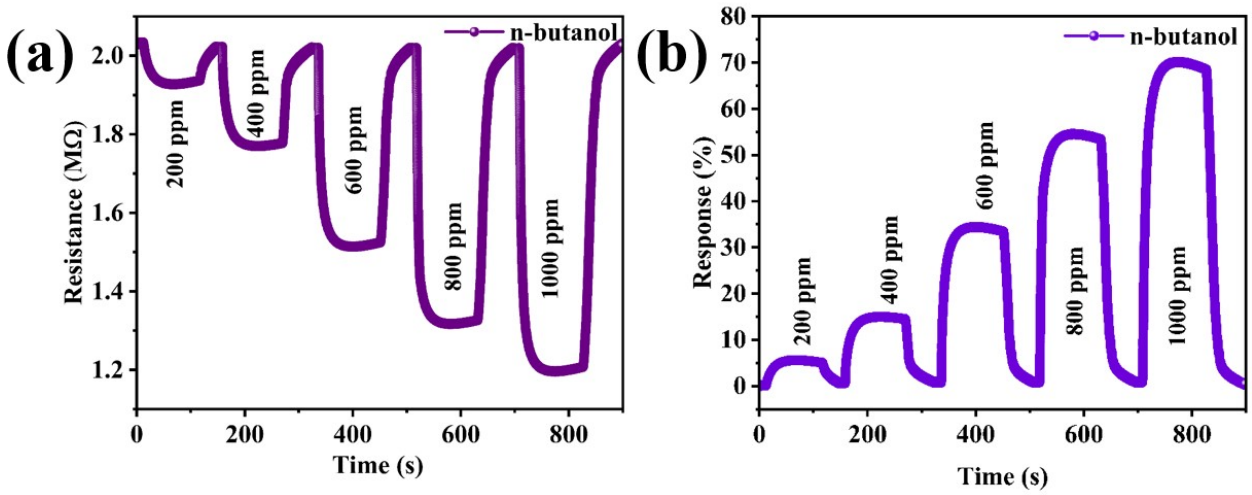

Fig. S3 Dynamic resistance study and their response of protocol#2 device towards n-butanol at different concentration.

Table: S1 Cross-sensitivity of the device protocol#2

Target gases concentration in mixture (ppm)		**Response (%)**
Toluene	n-butanol	
200	200	9
400	400	26
600	600	104
800	800	189
1000	1000	279